LASER INTERFEROMETER GRAVITATIONAL WAVE OBSERVATORY
- LIGO -
CALIFORNIA INSTITUTE OF TECHNOLOGY
MASSACHUSETTS INSTITUTE OF TECHNOLOGY

**Technical Note** **LIGO-T1900270-v1-** Date: 2019/05/10

# SAMS: Compression Fit mirror (CFM) thermal requirement modeling

Huy Tuong Cao, Sebastian Ng, Peter Veitch
*University of Adelaide*

**California Institute of Technology**
**LIGO Project, MS 18-34**
**Pasadena, CA 91125**
Phone (626) 395-2129
Fax (626) 304-9834
E-mail: info@ligo.caltech.edu

**Massachusetts Institute of Technology**
**LIGO Project, Room NW17-161**
**Cambridge, MA 02139**
Phone (617) 253-4824
Fax (617) 253-7014
E-mail: info@ligo.mit.edu

**LIGO Hanford Observatory**
**Route 10, Mile Marker 2**
**Richland, WA 99352**
Phone (509) 372-8106
Fax (509) 372-8137
E-mail: info@ligo.caltech.edu

**LIGO Livingston Observatory**
**19100 LIGO Lane**
**Livingston, LA 70754**
Phone (225) 686-3100
Fax (225) 686-7189
E-mail: info@ligo.caltech.edu

http://www.ligo.caltech.edu/

# Contents

**1 Introduction** **2**

**2 Identifying thermal effects** **2**

**3 Modeling method** **2**

**4 A baseline model** **2**

**5 Vertical shift of bottom mass** **4**

5.1 Vertical shift due to thermal dependent properties of suspension wires . . . . 4

5.2 Vertical shift due to thermal expansion of aluminium disc . . . . . 6

**6 Change in pitch due to shift in centre of mass** **7**

6.1 Single pendulum . . . . . 8

6.2 Double pendulum suspension . . . . . 11

# 1 Introduction

Compression Fit Mirrors (CFM) have been previously demonstrated as a potential adaptive optics for improving mode matching in future upgrades. These mirrors rely on the difference between thermal expansion coefficients of fused silica mirrors and aluminium actuating ring to actuate on mirror's surface deformation. CFM's therefore require heating, either by radiative or contact heater to perform as an adaptive optics. In this document, we identify the effects of heated adaptive optics on SAMS suspension architecture and therefore deduce thermal requirements for the system.

# 2 Identifying thermal effects

Figure 1 summaries the thermal effects of the CFM on the rest of SAMS suspension architecture and how they may limit limit SAMS performance. The three main effect identified due to heating of CFM are listed and discussed here:

1. **Vertical shift of second stage**: As the CFM heats up, heat will conduct out to suspension wires, causing suspension wires to expand. Furthermore, Young's modulus of steel generally decreases with increasing temperature, resulting in a lower effective spring constant of suspension wire. These combined effects cause suspension wires to lengthen thus lower bottom stage. The third effect is radial thermal expansion of actuating ring, which results in a slanting angle $\Omega_T$ between suspension wire and the vertical. This increase in angle $\Omega_t$ causes an updward shift in position of the bottom stage.

2. **Coupling to tilt due to shift in CFM centre of mass (COM)**: In cold state, CFM is bent convexly in shape. As the optics heat up, this convexity reduces, thus resulting in a shift in center of mass along the longitudinal direction.This shift in COM couples strongly to the suspension as a change in tilt.

3. **Effect on performance of dithering coil**: Heating of CFM is most likely to affect the performance of dithering voice coils within the vicinity of the CFM. Increase in temperature of magnets mounted on CFM can result in their reduction in magnetisation and therefore magnetic moment per unit volume, thus lowers the magnetic coupling between magnets and dithering coils. Surface-to-surface radiation between CFM, heater and dithering voice coil can also raise the temperature of the coil during operation, risking outgassing.

# 3 Modeling method

A combination of finite element analysis (FEA, e.g COMSOL) and analytical derivation will be used to model effect of thermal effects. FEA will output parameters describing CFM at steady-state heated state, including its temperature and deformations. These quantities will be fed into couplings, which will derived analytically (apart from calculation of force

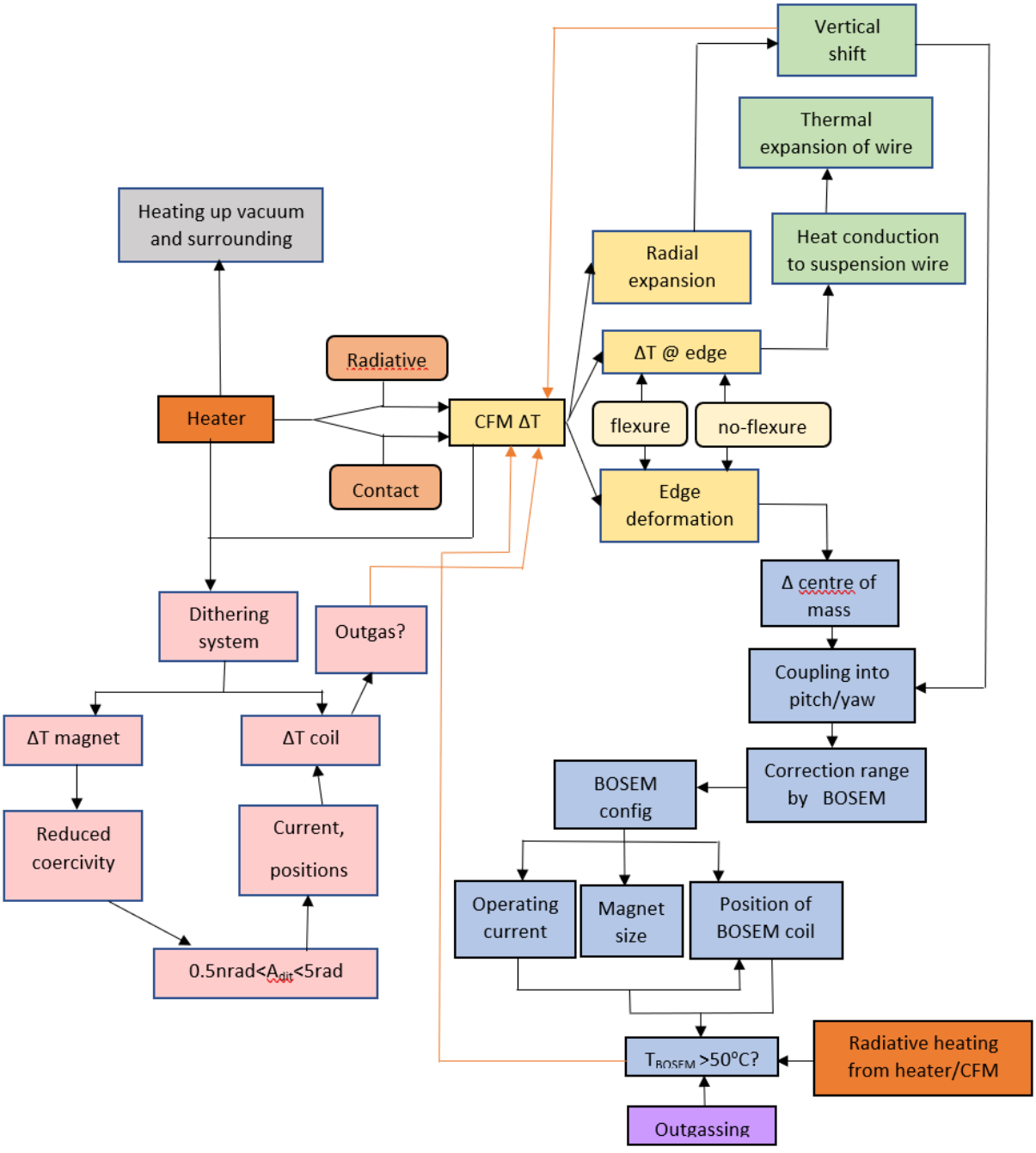


Figure 1: Identification of thermal effects on SAMS suspension architecture

| Symbol | Parameter | Value |
|---|---|---|
| | Lower stage | |
| $m_2$ | Bottom stage mass | 1 kg |
| $\varnothing_M$ | CFM's outer diameter | 120 mm |
| $t_R$ | Thickness of actuating ring | 38.8 mm |
| $dz$ | Actuating ring offset from mirror's barrel | -1.1 mm |
| $t_M$ | Mirror's thickness | 6 mm |
| $d_2$ | Distance between initial COM $x_n$ to the line joining suspension points | 0 mm |
| $s_3$ | x-displacement of suspension points from COM | 30 mm |
| $\Omega_2$ | Angle between suspension wire and vertical | 0 rad |
| | Upper stage | |
| $m_2$ | Top stage mass | 0.5 kg |
| $d_0$ | Distance between COM $x_m$ to the upper suspension point | 15 mm |
| $d_1$ | Distance between COM $x_m$ to the line joining lower suspension points | 15 mm |
| $s_2$ | x-displacement of lower suspension points from COM | 30 mm |
| $\Omega_1$ | Angle between upper suspension wire and vertical | 0 rad |
| | Suspension | |
| $l_2$ | Length of bottom stage suspension wire | 150 mm |
| $\varnothing_{\mathbf{wire}}$ | Suspension wire cross sectional diameter | 127 $\mu$m |
| | Temperatures | |
| $T_h$ | Maximum CFM temperature | 60°C |
| $T_a$ | Ambient temperature | 20°C |
| | Material properties | |
| | Steel wire | |
| $E_0$ | Young's modulus at room temperature | 210 GPa |
| $\partial E_T$ | Thermal coefficient for Young's modulus | -3.02e-4 1/K |
| $\alpha$ | Thermal expansion coefficient of steel wire | 12e-6 1/K |

Table 1: Table of parameters used in a baseline SAMS design

acting on magnets in BOSEM and dithering coils, in which complicated integrals will be numerically evaluated either with Matlab or Mathematica).

# 4 A baseline model

In order to testing various derived couplings in this document, we use a simple baseline model with a simple CFM at the bottom stage without no flexure holder and a mass of 1 kg. CFM's dimension has been selected to satisfy actuation and tensile stress requirement (see E1900126). The lower stage use 4 wire suspension, and upper stage use 2 wire suspension. The parameters and definition of these parameters are given in table 1 and figure 2.

# 5 Vertical shift of bottom mass

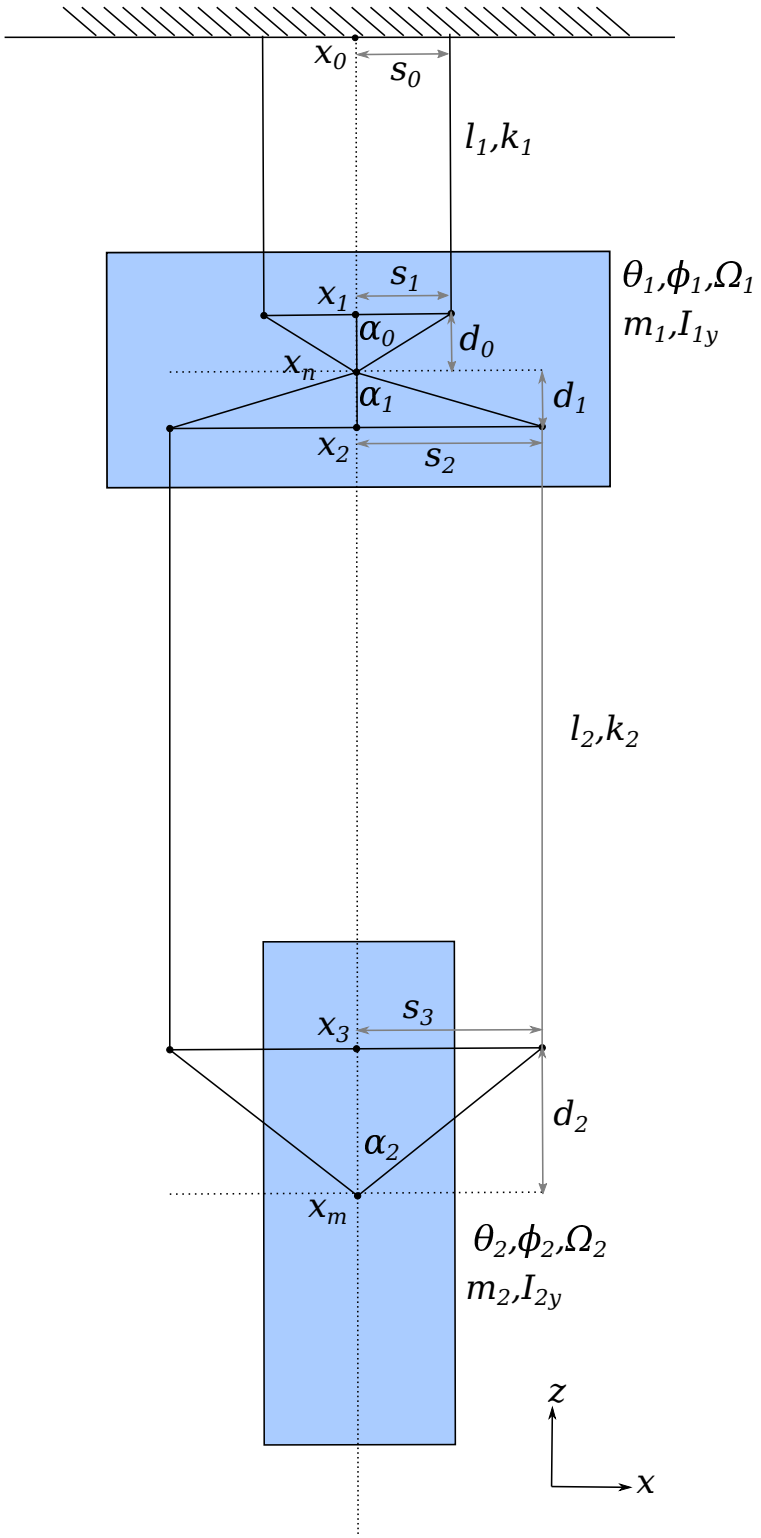


Figure 2: Schematics of double pendulum suspension from the side

### 5.1 Vertical shift due to thermal dependent properties of suspension wires

The two main thermal properties that affect the length of suspension wires are thermal expansion of steel wire and temperature-dependent Young's modulus. Young's modulus dependence on temperature of steel is presented by a phenomenological exponential function from [1]:

$$E(\Delta T) = E_0 \exp\left[-\frac{1}{2}\left(\frac{\Delta T}{e_3}\right)^{e_1} - \frac{1}{2}\left(\frac{\Delta T}{e_4}\right)^{e_2}\right] \tag{1}$$

where $e_1 = 3.768,\ e_2 = 1,\ e_3 = 639°\text{C},\ e_4 = 1650°\text{C}$ and $\Delta T$ is the change in temperature from 20°C. The region between $\Delta T = 0$ to 40 K can be well approximated by a linear function of the form:

$$E(\Delta T) = E_0\,(1 + \partial E_T \Delta T) \tag{2}$$

In order to evaluate the stretch in the wire by these thermal effects. We first needs to obtain the temperature profile for a suspension wire heated from one end. Assuming the upper stage is large with large surface area and is far away from the bottom stage where the heat source is installed, its temperature with be approximately constant at ambient temperature $T_a$. In equilibrium, due to high thermal conductivity of both aluminium and steel wires, the heated end of fibre will be at the same temperature as the actuating ring. Here, we assume an upper limit of $T_h = 60°\text{C}$. Thus we define $\delta T = T_h - T_a$ as the difference in temperature between the two ends of the wire. Furthermore, with high thermal conductivity of steel, heat conduction is assumed to be the dominating process when compared to radiation. The temperature profile along the wire is therefore simply described by a linear equation:

$$T(x) = \frac{\delta T}{l}x + T_a \tag{3}$$

where $x$ is distance from the wire's cold end at the upper stage. Now to solve for the stretch of the wires, we consider Hooke's law which relate stress and strain, in which we include thermal strain caused by thermal expansion:

$$\begin{aligned} \sigma &= E(\epsilon - \alpha\Delta T) \\ \therefore \frac{mg}{4A} &= E_0(1 + \partial E_T \Delta T(x))\left(\frac{du}{dx} - \alpha\frac{\delta T}{l}x\right) \end{aligned} \tag{4}$$

where $u$ is displacement along $x$-axis, $A$ is the cross-sectional area a steel wire and 1/4 in stress accounts for the load's being shared between four suspension wires

Equation 4 can be re-arranged and integrated to obtain the displacement of the wire:

$$\Delta l = \frac{mg}{4AE_0}\int_0^l dx \frac{1}{1 + \partial E_T \frac{\delta T}{l}x} + \alpha\int_0^l dx \frac{\delta T}{l}x \tag{5}$$

An expression for the stretching of the wire can then be simply derived to be:

$$\Delta l = \frac{mg}{4AE_0}\frac{l}{\partial E_T \delta T}\ln\left(1 + \partial E_T \delta T\right) + \frac{\alpha \delta T l}{2} \tag{6}$$

For our baseline design, suspension wires at T=60°C experiences in a stretch of 175 $\mu$m, in which 139 $\mu$m change is caused by temperature-dependent Young's modulus.

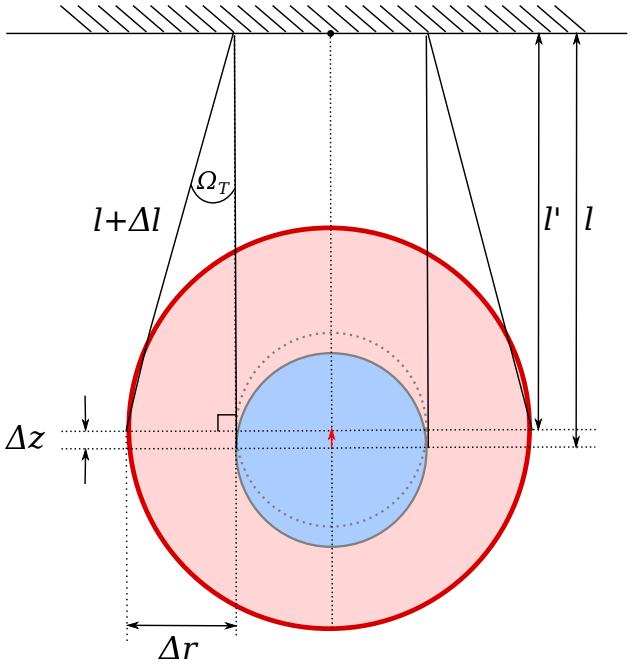


Figure 3: Front view of a suspended CFM as it is heated up (not to scale). Radial expansion creates and angle between suspension wire and the vertical, effectively shortens the wire and shift the suspended optics upward

### 5.2 Vertical shift due to thermal expansion of aluminium disc

FEA model shows that as the CFM heats up, the radius of a 120 mm OD CFM can change up to 56 $\mu m$ at $\Delta T = 40$ K. This would create a small angle $\Omega_T$ between a suspension wire and the vertical (see figure 3). Consider a baseline design in which the mirror is suspended vertically in its cold state. As the radius changes by $\Delta r$, the distance $l'$ can be found from $l + \Delta l$ and initial wire's length $l$:

$$l' = \sqrt{(l + \Delta l)^2 - \Delta r^2} \tag{7}$$

and the shift $\Delta z$, which is the overall shift due to both wire extension and CFM radial expansion, is the difference between $l'$ and $l$. Using $\Delta z = 56\mu$m and $l = 150$mm, we found $\Delta z = -174.986\mu$m, which means the dominating effect is still due to wire extension discussed in previous section. Radial expansion only shifts the mass upward by 10.5 nm.

Notice that the radial change at different positions along the barrel of the optics will vary. There is a 2.1 nm difference in upward shift between the front and back of a 1kg 120-mm-OD CFM, whose barrel length is approximate 40 mm. This difference will thus couple through as a change in pitch of a reflected beam , which is estimated to be 107 nrad at $\Delta T = 40$K. This change in pitch is much smaller than that caused by shift in optics' centre of mass, which will be discussed subsequently.

In conclusion, for our baseline design, we expect a sag in suspended CFM's position of approximately 175 $\mu$m at $\Delta T = 40$K. For a nominal 1 m ROC mirror, this implies a change in pitch of 350 $\mu$rad for beam reflected off the CFM.

# 6 Change in pitch due to shift in centre of mass

## 6.1 Single pendulum

The change in convexity of CFM with increasing temperature results in shift of its COM along the optical axis ($x$-axis in figure 4) from $x_n$ to $x_n' = x_n + \Delta x$. Assuming that the CFM is suspended symmetrically from it COM at cold state at distance $r$. The mass can be divided into two equal halved with masses $m_1 = m_2 = m/2$ of effective thicknesses of $t/2$. Therefore, the position of a CFM in its cold state can be given by:

$$\begin{aligned} x_n &= \frac{m_1 x_{m1} + m_2 x_{m2}}{m} \\ &= \frac{1}{2m}\left[m x_{m_1} + m\left(x_{m1} + \frac{t}{2}\right)\right] \\ &= x_{m1} + \frac{t}{2} \end{aligned} \tag{8}$$

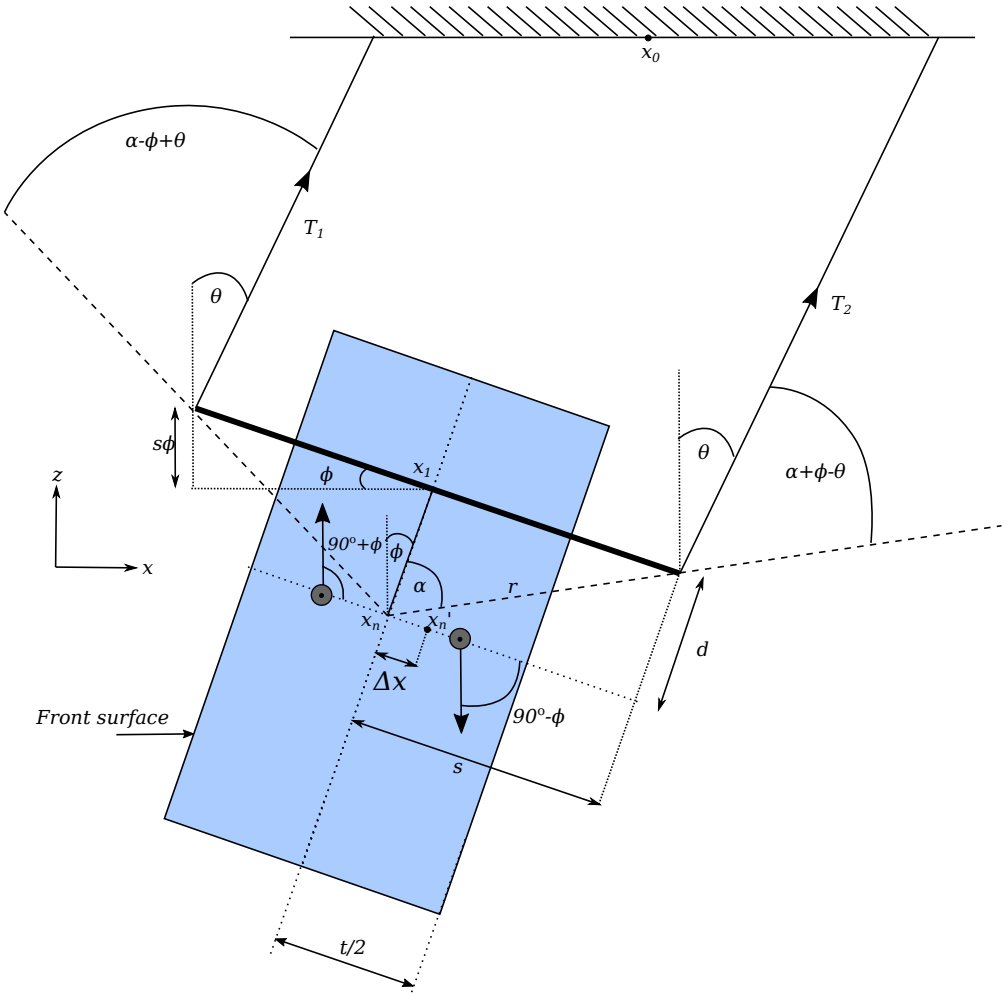


Figure 4: Side view of a cylindrical mass in with tilt and longitudinal motion in an single pendulum suspension

Now consider that CFM's COM shifts to more positive $x$ by $\Delta x$ at some temperature $T > T_{\text{ambient}}$. This would be equivalent to adding some extra mass $\Delta m$ onto one half of the initial mass and removed the same amount of $\Delta m$ from the other half. We can then find an expression for this $\Delta m$ in term of $\Delta x$:

$$\begin{aligned} x_n' &= \frac{(m/2 - \Delta m)x_{m1} + (m/2 + \Delta m)(x_{m1} + t/2)}{m} \\ &= x_n + \frac{\Delta m t}{2m} = x_n + \Delta x \\ \therefore \Delta m &= \frac{2m\Delta x}{t} \end{aligned} \tag{9}$$

We can thus treat the effect of shift in CFM's COM as applying two equal but opposing forces at the COM's of the mass' two halve at $t/4$ from $x_n$:

$$F_1 = \frac{2mg\Delta x}{t}\hat{z} \tag{10}$$

$$F_2 = -\frac{2mg\Delta x}{t}\hat{z} \tag{11}$$

The two forces cancel one another out but provide a torque that tilts the mass around $y$-axis:

$$\begin{aligned} \Sigma\tau_y &= -mg\frac{\Delta x}{2}\left[\sin\left(\frac{\pi}{2} + \phi\right) + \sin\left(\frac{\pi}{2} - \phi\right)\right] \\ &= -mg\Delta x\cos\phi \simeq mg\Delta x\left(1 - \frac{\phi^2}{2}\right) \end{aligned} \tag{12}$$

We can write down the equations of motion (e.o.m) for tilt and longitudinal motions of the a mass in single pendulum suspension, following Calum Torrie's formulation in [2]:

$$m\ddot{x}_n = -\frac{mg}{l\cos\Omega}(x_n - x_0) + \frac{mgd}{l\cos\Omega}\phi \tag{13}$$

$$I_y\ddot{\phi} = \frac{mgd}{l\cos\Omega}(x_n - x_0) - \left(mgd + \frac{mgd^2}{l\cos\Omega} + \frac{mgs^2\sin^2\Omega}{l\cos\Omega} + 2ks^2\cos^2\Omega\right)\phi \tag{14}$$

where the parameters in used are:

$l$ = the length of a wire

$\Omega$ = angle formed between suspension wire with the vertical in $zy$-plane, assumed to be zero for baseline design

$k$ = spring constant of suspension wire

$s = r\sin\alpha$ = the half separation of 2 wires in x-direction

$d = r\cos\alpha$ = the distance the wires break-off above the line through COM

$x_0$ = the midpoint of the line joining two suspension wires in x-direction

with $\Omega = 0$, equations 13 and 14 are simplified to:

$$m\ddot{x}_n = -\frac{mg}{l}(x_n - x_0) + \frac{mgd}{l}\phi \tag{15}$$

$$I_y\ddot{\phi} = \frac{mgd}{l}(x_n - x_0) - \left(mgd + \frac{mgd^2}{l} + 2ks^2\right)\phi \tag{16}$$

Since there is no forces acting on the mass longitudinally:

$$\Sigma F = 0 = -\frac{mg}{l}(x_n - x_0) + \frac{mgd}{l}\phi$$
$$x_n = x_0 + d\phi \tag{17}$$

If $d = 0$, then tilt and longitudinal motion become uncoupled.

The shift in COM results in a torque acting on the suspended mass as discussed above. The e.o.m for tilt then becomes:

$$\Sigma\tau = -mg\Delta x\left(1 - \frac{\phi^2}{2}\right) = \frac{mgd^2}{l}\phi - \left(mgd + \frac{mgd^2}{l} + 2ks^2\right)\phi$$
$$\therefore \phi = \frac{1}{\Delta x}\left[-\left(d + \frac{2ks^2}{mg}\right) + \sqrt{\left(d + \frac{2ks^2}{mg}\right)^2 + 2\Delta x^2}\right] \tag{18}$$

Had we used the first order approximation of $\cos\phi = 1$ for small angle, $\phi$ could have been found as:

$$\phi = \frac{\Delta x}{d + \frac{2ks^2}{mg}} + \mathcal{O}\left(\Delta x^3\right) \tag{19}$$

By performing Taylor series expansion of the square-root term in expression 18, equation 19 can be obtained:

$$\sqrt{\left(d + \frac{2ks^2}{mg}\right)^2 + 2\Delta x^2} \simeq d + \frac{2ks^2}{mg} + \frac{\Delta x^2}{d + \frac{2ks^2}{mg}} + \mathcal{O}\left(\Delta x^4\right) \tag{20}$$

Sanity check of expression 19 reveals expected physical behaviours:

- As $k \to \infty$ (suspension wire becomes highly stiff), there is no tilt of the optics
- As $s \to \infty$ (suspension points are far away COM), tilt also reduces
- As $m \to 0$ (mass of suspended optics becomes smaller), tilt also reduces

### 6.2 Double pendulum suspension

SAMS suspension would be a two-stage suspension. The e.o.m's for longitudinal and tilt motion of a double pendulum are:

$$m_1\ddot{x}_n = -(m_1+m_2)g\theta_1 + m_2 g\theta_2 \tag{21}$$

$$m_2\ddot{x}_m = -m_2 g\theta_2 \tag{22}$$

$$\begin{aligned} I_{1y}\ddot{\phi_1} = &-(m_1+m_2)gd_0(\phi_1-\theta_1) - 2k_1 s_0^2\cos^2\Omega_1\phi_1 - m_2 g d_1(\phi_1-\theta_2) \\ &- 2k_2 s_2^2\cos^2\Omega_2(\phi_1-\phi_2) - \frac{(m_1+m_2)gs_0\sin^2\Omega_1}{l_1\cos\Omega_1}\phi_1 \\ &- \frac{m_2 g s_2^2\sin^2\Omega_2}{l_2\cos\Omega_2}(\phi_1-\phi_2) \end{aligned} \tag{23}$$

$$I_2\ddot{\phi_2} = -m_2 g d_2(\phi_2-\theta_2) - 2k_2 s_2^2\cos^2\Omega_2(\phi_2-\phi_1) - \frac{m_2 g s_2\sin^2\Omega_2}{l_2\cos\Omega_2}(\phi_2-\phi_1) \tag{24}$$

where:

$$\theta_1 = \frac{x_n - x_0 - \phi_1 d_0}{l_1\cos\Omega_1} \tag{25}$$

$$\theta_2 = \frac{x_m - x_n - \phi_2 d_2 - \phi_1 d_1}{l_2\cos\Omega_2} \tag{26}$$

The parameters used are defined in figure 2

For SAMS suspension, the top stage will be a single loop suspension and the e.o.m's for tilt and longitudinal motion (equations 21 to 23) can be rewritten in the form of matrix of coupled equations:

$$\begin{bmatrix} 0 \\ -m_2 g\Delta x\frac{s_2}{s_3} \\ 0 \\ -m_2 g\Delta x \end{bmatrix} = \begin{bmatrix} k_{11} & k_{12} & k_{13} & k_{14} \\ k_{21} & k_{22} & k_{23} & k_{24} \\ k_{31} & k_{32} & k_{33} & k_{34} \\ k_{41} & k_{42} & k_{43} & k_{44} \end{bmatrix} \begin{bmatrix} x_n \\ \phi_1 \\ x_m \\ \phi_2 \end{bmatrix} \tag{27}$$

and $k_{ij}$ coefficients are given as following:

$$
\begin{aligned}
k_{11} &= -\frac{(m_1+m_2)g}{l_1\cos\Omega_1} - \frac{m_2 g}{l_2\cos\Omega_2}, k_{12} = \frac{(m_1+m_2)gd_0}{l_1\cos\Omega_1} - \frac{m_2 g d_1}{l_2\cos\Omega_2} \\
k_{13} &= \frac{m_2 g}{l_2\cos\Omega_2}, k_{14} = -\frac{m_2 g d_1}{l_2\cos\Omega_2}, k_{21} = \frac{(m_1+m_2)gd_0}{l_1\cos\Omega_1} - \frac{m_2 g d_1}{l_2\cos\Omega_2} \\
k_{22} &= -(m_1+m_2)gd_0\left(1+\frac{d_0}{l_1\cos\Omega_1}\right) - m_2 g d_1\left(1+\frac{d_1}{l_2\cos\Omega_2}\right) \\
&\quad - 2k_2 s_2^2\cos^2\Omega_2 - \frac{m_2 g s_2^2\sin^2\Omega_2}{l_2\cos\Omega_2} \\
k_{23} &= \frac{m_2 g d_1}{l_2\cos\Omega_2}, k_{24} = \frac{m_2 g(d_1 d_2 + s_2^2\sin^2\Omega_2)}{l_2\cos\Omega_2} + 2k_2 s_2^2\cos^2\Omega_2 \\
k_{31} &= \frac{m_2 g}{l_2\cos\Omega_2}, k_{32} = \frac{m_2 g d_1}{l_2\cos\Omega_2}, k_{33} = -\frac{m_2 g}{l_2\cos\Omega_2}, k_{34} = \frac{m_2 g d_2}{l_2\cos\Omega_2} \\
k_{41} &= \frac{m_2 g d_2}{l_2\cos\Omega_2}, k_{42} = -\frac{m_2 g d_2 d_1}{l_2\cos\Omega_2} + 2k_2 s_2^2\cos^2\Omega_2 + \frac{m_2 g s_2\sin^2\Omega_2}{l_2\cos\Omega_2} \\
k_{43} &= \frac{m_2 g d_2}{l_2\cos\Omega_2}, k_{44} = -\frac{m_2 g d_2^2}{l_2\cos\Omega_2} - 2k_2 s_2^2\cos^2\Omega_2 - \frac{m_2 g s_2\sin^2\Omega_2}{l_2\cos\Omega_2}
\end{aligned}
\tag{28}
$$

This system of equations can be solved for change in longitudinal translation and tilt of each mass, albeit being rather complicated. The baseline model assumes that $\Omega_1 = \Omega_2 = 0$ , $d_2 = 0$. The four degress of freedom that describe tilt and longitudinal motion of the system is then solved to be:

$$x_n = \Delta x \frac{d_0 m_2(s_2+s_3)}{s_3(d_0 m_1 + d_0 m_2 + d_1 m_2)} \tag{29}$$

$$\phi_1 = \Delta x \frac{m_2(s_2+s_3)}{s_3(d_0 m_1 + d_0 m_2 + d_1 m_2)} \tag{30}$$

$$x_m = \Delta x \frac{m_2(d_0 s_2 + d_0 s_3 + d_1 s_2 + d_1 s_3)}{s_3(d_0 m_1 + d_0 m_2 + d_1 m_2)} \tag{31}$$

$$\phi_2 = \frac{\Delta x m_2(d_0 g m_1 s_3 + d_0 g m_2 s_3 + d_1 g m_2 s_3 + 2k_2 s_2^3 + 2k_2 s_2^2 s_3)}{2k_2 s_2^2(d_0 m_1 + d_0 m_2 + d_1 m_2)} \tag{32}$$

For $s_2 = s_3$, these equations reduce to:

$$x_n = 2\Delta x \frac{d_0 m_2}{d_0 m_1 + d_0 m_2 + d_1 m_2} \tag{33}$$

$$\phi_1 = 2\Delta x \frac{m_2}{d_0 m_1 + d_0 m_2 + d_1 m_2} \tag{34}$$

$$
\begin{aligned}
x_m &= 2\Delta x \frac{m_2(d_0 + d_1)}{d_0 m_1 + d_0 m_2 + d_1 m_2} \\
&= x_n + \frac{2\Delta x m_2 d_1}{d_0 m_1 + d_0 m_2 + d_1 m_2}
\end{aligned}
\tag{35}
$$

$$\phi_2 = \frac{\Delta x m_2(d_0 g m_1 + d_0 g m_2 + d_1 g m_2 + 4k_2 s_2^2)}{2k_2 s_2^2(d_0 m_1 + d_0 m_2 + d_1 m_2)}$$

$$= \frac{\Delta x m_2 g}{2k_2 s_2^2} + \phi_1 \tag{36}$$

A few key points observed here are:

- Tilt angle of bottom stage optics are sum of upper stage tilt as well as tilt caused by the shift in CFM COM in the single pendulum suspension
- Greater vertical separation between suspension points of upper and lower sets of wires reduce the coupling of COM shift from lower stage to upper stage
- As the upper stage increases in mass, it effectively becomes stiffer and less susceptible to tilt and longitudinal motion caused by shift in COM of bottom stage
- If $d_0 = 0$ (i.e. the suspension point of the upper stage is at its centre of mass) then there is no longitudinal change of upper mass as it is pivoted at its COM.

The shift in COM of a CFM is linear with its change in temperature. For the baseline design, FEA model shows that this shift can be described as a linear function $\Delta x = 0.71[\mu m/K]\Delta T$. At $T = 60°$C, $\Delta x = 28.4\mu m$ from its cold state.

Since the bottom stage has 4 wire suspension architecture, $k_2$ would become $2k_2$. The change in tilt of the bottom stage is dominated by the induced change in top stage:

$$\phi_1 = 1.52\text{mrad}$$
$$\phi_2 = 4.4\mu\text{rad} + \phi_1$$

The longitudinal change of each stage is:

$$x_n = 22.8\mu m$$
$$x_m = 45.6\mu m$$

The new COM $x'_m$ is therefore $74\mu m$ relative to $x_0$. At $T = 60°$, the mirror's front surface is 23.0095 mm from its COM, compared to 23.046 mm at $T = 20°$. The mirror's front surface thus has shifted longitudinally by $74\mu$m-($46\mu$m - $9.5\mu$m) = 37.5 $\mu$m

# References

[1] M. Seif, J. Main, J. Weigand, F. Sadek, L. Choe, C. Zhang, J. Gross, W. Luecke, and D. McColskey, "Nist Technical Note 1907: Temperature-dependent material modeling for strutural steels: formulation and application," Tech. Rep. 1907, National Institute of Standards and Technology, April 2016.

[2] C. Torrie, *Development of Suspension for the GEO 600 Gravitaional Wave Detector*. PhD thesis, Department of Physics and Astronomy, University of Glasgow, 2000.